Al-Qadisiyah JournalFor Engineering Sciences 18 (2025) 378 – 390

Contents lists available at: http://qu.edu.iq

Al-Qadisiyah Journal for Engineering Sciences

Journal homepage: https://qjes.qu.edu.iq

Research Paper

Improving the performance of a photovoltaic panel using phase change materials enhanced with metal foams

Khaldi Sabrina [1]✉, ***Driss Nehari*** [2], ***Abdelkader Youcefi***[1], ***and Bachir Imin*** [1]

[1]*Laboratory of Aeronautics and Propulsion Systems, University of Sciences and Technology in Oran (USTO), Oran 31000, Algeria.*
[2]*Laboratory of Applied Hydrology and Environment, Faculty of Science and Technology, University of Ain Temouchent, Ain Temouchent 46000, Algeria.*

ARTICLE INFO

Article history:
Received 01 June 2025
Received in revised form 21 August 2025
Accepted 12 November 2025

keyword:
Phase change material
Photovoltaic panel
Thermal control
PV cooling
Metal foam
Economic study

ABSTRACT

A numerical investigation is conducted to improve the overall performance of a photovoltaic (PV) system using phase change materials (PCMs) reinforced with different types of foam materials. The PV panel was modelled as an aluminium plate in contact with a rectangular cavity filled with PCM with or without foam. The impact of the melting point of PCMs, as well as the effect of adding (Cu), (Al), and (SiC) foam to RT25 on the cooling performance of the PV, was analyzed. The results showed that the melting point of MCPs affected the PV temperature, where RT25 reduced 10.7 °C compared to RT44, and the addition of foam to PCM with a porosity of 97% and an air permeability index (IPP) of 5 is the most optimal in this system. such as the use of Cu as foam allows an improvement of 16.18% compared to standard PV and 12% compared to the use of PCM alone. This work also highlights the positive impact of improving PV efficiency on economic and environmental aspects. Where the $(PV/PCM(RT25) + foam(SiC))$ combination is a high-performance and more economical solution. On the other hand, the proposed cooling system can increase energy production by 24 $(kWh/m^2/year)$ and reduce CO_2 emissions by up to 48 $(kg/m^2/year)$.

1. Introduction

Electricity production is a major issue due to demographic changes and the development of certain regions. This trend suggests a significant increase in energy consumption. A large portion of global energy production comes from fossil resources, which result in two main problems: the depletion of reserves and environmental pollution caused by toxic waste, as well as the dangers posed by nuclear power plants, which represent threats to humanity and the ecosystem of our planet. In this context, it is urgent for humanity to transition to renewable energy sources to meet its needs. Solar energy stands out for its many advantages, such as its wide accessibility, safety, stability, and immense potential. Photovoltaic cells are capable of directly converting sunlight into electricity. However, their efficiency can be compromised by the excessive heat they generate. Indeed, when they heat up, their performance decreases[1]. Typically, fewer than 20% of the solar energy captured is converted into electrical energy; the remainder is converted into thermal energy. This thermal energy elevates the operational temperature of photovoltaic systems, consequently diminishing their longevity and efficiency [2]. Research conducted by Othman et al. [3] indicates that an increase of 1 °C in temperature leads to a reduction in the efficiency of conventional silicon solar panels by 0.4 to 0.5%. According to another study, the efficiency of older PVs might drop by as much as 0.69% for every degree Celsius [4]. Additionally, researchers are looking for novel ways to raise PV conversion efficiency. These methods must meet strict requirements like uniform PV temperature, low cost, long durability, and ease of installation. To address this issue, several innovative solutions are being explored. Among them, the integration of passive and active cooling systems, with the latter requiring no energy source to operate. Among the approved mechanisms in passive cooling of PVs, it is to transfer excess heat naturally by buoyancy forces to the ambient air. Generally speaking, components like fins, ribs, and baffles [5,6] are employed to enhance the exchange surface and hence boost the efficiency of natural convection. Applying liquid or gel layers [7] in place of air around the solar cell [8] or submerging the panel in water [7] are two more methods to enhance natural convection. Unlike passive cooling, active cooling systems use means such as pumps and accelerators to circulate heat transfer fluids designated to cool PVs, but these techniques can result in a non-uniform cooling effect [9]. This thermal imbalance can cause structural failures and reduce conversion efficiency. In order to mitigate these issues, methodologies such as the implementation of heat sinks, heat spreaders, and phase change materials (PCMs) are employed [10]. Generally, active cooling methodologies demonstrate superior efficiency compared to passive techniques, however, they are characterized by significantly higher costs and increased complexity [11]. In the recent past, the volume of scholarly articles published pertaining to PCMs in the year 2022 is projected to be approximately 10,479 articles [12]. Various research niches have tested the performance of PCMs in their respective fields. Among these, in the construction and building sectors, PCMs are mainly used for components such as concrete, bricks, walls, floors, roofs, and windows. In the biomedical field, they are used for applications such as vaccine transport boxes and newborn coolers [12]. PCMs are utilized not only in air conditioning cycles [13], but also in thermal storage systems [14] for the recovery of waste heat. Recently, research [2, 15] suggested the use of PCMs for passive cooling of PVs. During heating times, PCMs can absorb surplus thermal energy from the cells because of their latent heat storage capability. As stated in Ref. [16], the PVT/PCM system increases system performance by 14% compared to PV/T. This is also reported by Elsheniti et al. [17].

*Corresponding Author.
E-mail address: sabrina.khaldi@univ-tiaret.dz ; Tel: (+213) 661-11 2679 (Khaldi Sabrina)

https://doi.org/10.30772/qjes.2025.161063.1581

Nomenclature

C_p	Specific heat, $(J/kg/k)$	u	velocity component in x-axis, (m/s)
C_f	Inertial coefficient	v	Velocity component in y-axis, (m/s)
dp	Foam pore diameter, (m)	$2d$	Two dimensional
df	Diameter of foam skeleton,(m)	*Greek Symbols*	
f_i	Liquid fraction	ρ	density, kg/m^3
g	Gravitational acceleration (m/s^2)	ε	porosity
h	Sensible enthalpy, (J)	μ	viscosity, Pas
H	Total enthalpy, (J)	β	Thermal expansion coefficient, $1/K$
ΔH	Fractional latent-heat, $(J/kg/k)$	η	Electrical efficiency
k	Thermal conductivity, $(W/m/K)$	*Subscripts*	
K	Permeability	$melt$	Melting
L	Latent heat, (J/kg)	eff	Effective
T	Temperature, (k)	ref	Reference
t	Time, (s)	l	Liquid
x,y	Cartesian coordinates, (m)	s	Solid

According to their findings, PV performance can be maximized with a 14.24% gain in electrical efficiency when PCM and PVT are combined. In a similar vein, Prabhu et al. [18] demonstrated that phase change materials (PCM) can substantially reduce the temperature of the system, achieving a decrease ranging from 3 to 26.6 °C, which in turn enhances the electrical efficiency of the module from 1% to 56%. Moreover, in their comparative analysis, Khanna et al. [19] found that the integration of the PV-PCM system resulted in a temperature reduction of 19 °C in the photovoltaic (PV) components, while simultaneously elevating the efficiency by a margin of 17.1% to 19% in contrast to the PV system operating independently. The efficacy of a bifluid photovoltaic/thermal collector utilizing paraffin, incorporating both air and water, was rigorously investigated by Awad et al. [20]. The findings indicated that the overall system efficiency increased from 59.01% to 80.29% when the PCM was used. It also reduced the energy consumption required to circulate the nanofluids compared to continuous cooling [21]. A novel paradigm for incessant electricity generation around the clock is the integration of photovoltaic (PV) technology with a thermoelectric generator (TEG) and phase change material (PCM), referred to as the PV-TEG-PCM system. This system harnesses photovoltaic energy during daylight hours, whereas the TEG capitalizes on the thermal gradient between the PV and PCM to facilitate electricity generation throughout the entire day. The role of PCM is to protect the PV against overheating during the daytime and increase the temperature difference during the nighttime. Wei et al. [22] conducted an experimental study on improving the performance of the hybrid system (PV-TEG-PCM) and optimizing its structure. They observed that this system showed excellent electrical performance, with an overall efficiency reaching up to 20.8%. PCMs generally have low thermal conductivity. The properties of thermal conductivity exert a significant influence on the efficiency of heat transfer mechanisms. Song Lv and colleagues [23] conducted an investigation into the implications of varying thermal conductivity values on the operational efficacy of the PV-TEG-PCM cooling system.The findings demonstrate that the PV-TEG-PCM system performs better when the PCM has a higher thermal conductivity, which drives researchers to explore solutions to improve it. Much research has been conducted to enhance free convection within PCMs by adding fins and copper and aluminum wires [24]. Among the contemporary methodologies employed in this domain is the amalgamation of phase change materials (PCM) and metallic foam. A systematic experimental inquiry conducted by Firoozzadeh et al. [25] analyzed the effects of integrating porous media into phase change materials on the thermal regulation efficiency of photovoltaic systems. The photovoltaic module's back was covered with two centimeter-thick layers of porous aluminum. The photovoltaic panels' temperature dropped by 14.5 °C, according to the results. However, according to Abdulmunem et al. [26], the temperature of PVs might drop by as much as 21.5 °C when PCMs are added to the system. Additionally, they suggested employing copper foam in the PCM as a passive cooling technique for PV. According to the data, this system's electrical efficiency increased by 5.68%, and its PV temperature decreased by 13.29% when compared to the PV+PCM scenario. Likewise, an experimental investigation of the impact of PCM in combination with copper and graphite was carried out by Hachem et al. [27]. It was shown that adding pure PCM to the PV system improved its electrical efficiency by an average of 3%, while adding PCM+metal foam enhanced it by 5.8%. A study by Alipour et al. [28] looked at how using nanofluids as the working fluid helped them understand how certain factors affected the thermal and electrical efficiency of the PVT/PCM system with copper foam. In the comparative analysis between the PVT/PCM configuration and the PVT/PCM+copper foam configuration, it was observed that the incorporation of copper foam into the PCM configuration substantially enhanced its thermal efficiency by 25.4% and augmented its electrical efficiency by 3.9%. Numerous studies examine how to optimize the metal foam's properties for low cost and high thermal performance. To improve the performance of a metal foam/PCM (MFPCM) composite and a PCM-based heat sink, Errebii et al. [29] studied how to improve the cooling system's settings and investigated the impacts of various metal foams (Cu, Al, and Ni). The results showed that the copper (Cu) MFPCM, the largest temperature drop was obtained with the best porosity of 93% or the best pore density of 20 PPI. Phase change materials, encompassing eutectic, inorganic, and organic variants, are readily accessible. Organic PCMs are frequently chosen as thermal energy storage materials due to their primary benefits, which include better chemical and thermal stability, wide availability over a range of temperatures, high latent heat of fusion, and resistance to corrosion [30]. However, these characteristics determine the lifetimes of PCMs; the most thermally stable PCM is. Organic phase change materials are then divided into paraffins and non-paraffins. Normal paraffins of the $C_nH_{(2n+2)}$ have almost the same properties, which belong to saturated hydrocarbons. The latent heat and melting temperature exhibit an augmentation concomitant with the escalation in the parameter 4 [31]. Paraffins are extensively utilized within thermal energy storage systems, attributed to their minimal subcooling characteristics and reduced vapor pressure in the molten state. They are also available commercially at a reasonable cost. These PCMs are non-toxic and ecologically safe [32]. Furthermore, multiple thermal cycles have demonstrated the strong thermal and chemical stability of paraffins [33]. In both technical and financial concerns, the PCM layer's thickness is crucial. In this context, the effect of PCM thickness on the performance of the PV-PCM system was examined by Tao Ma et al. [34] examined the influence of phase change material (PCM) thickness on the operational efficacy of the photovoltaic-phase change material (PV-PCM) system in this context. The results indicate that the duration of melting is prolonged by approximately 10 minutes on average for each 5 *mm* increment in thickness. The PCM may, however, occasionally function as a thermal resistor to dissipate heat to the PV panel's back, raising the PV's temperature. When the PCM temperature falls below the melting point during the winter, this event may happen. This scenario emphasizes how crucial it is to choose PCM thickness appropriately based on regional climate conditions. Ultimately, the goal of this study is to cool the PV and attain a consistent temperature throughout the PV's whole surface. To enhance its electrical efficacy and longevity. Few studies have examined the impact of the PV/PCM+MF cost while improving efficiency. In this context, we propose to carry out an already validated transient numerical study using the enthalpy-porosity method aimed at optimizing the photovoltaic (PV) module's integration settings for phase change materials (PCM) by themselves and in combination with metal foam; the geometric model and the method followed for the numerical solution are presented in detail. The objective of this article is to carry out a numerical study on PV/PCM and PV/PCM+MF cooling systems to optimize their parameters in order to minimize the associated costs while maximizing their efficiency. Various sources [2, 34–36] show that the physical model simplifies the PV module to an aluminum plate. Glass, PV cells, ethylene-vinyl acetate (EVA), and Tedlar-Polyester-Tedlar (TPT) are the usual components of a photovoltaic module [34]. There could be noticeable changes if the photovoltaic module is reduced to an aluminum plate. However, Tao Ma et al. [34] examined the impact of this simplification. The results show that the average temperature difference between the two profiles is only around $\pm$ 1.5 °C. Thus, this study comes to the conclusion that the aluminum plate version of the reduced PV module is acceptable. Based on our knowledge and review of existing works, few studies have explored the effects of foam geometric parameters and the nature of the foam embedded into the PCM for thermal management of photo-

voltaic panels. For the first time, this study combines and analyzes the effect of several key parameters directly influencing the performance of the PV system. It particularly examines the impact of the PCM melting temperature (i.e., type of paraffin), foam type (metallic and non-metallic), as well as the porosity and pore density. The objective is to optimize the performance of the photovoltaic panel in a cost-effective manner in terms of efficiency and cost. The work is organized as follows. First, we will examine the effect of the PCM melting temperature, i.e., the nature of PCM such as RT25, RT35, and RT44, on the performance of the PV system. Then, the best type of PCM will be selected to be combined with different types of foam (copper, aluminium, and silicon carbide) to determine the appropriate foam based on its thermal efficiency and cost. Jiang et al. [36] found that the stability of phase change materials (PCMs) is enhanced by the incorporation of porous media, which act as shape stabilizers, preventing leakage and maintaining the structural integrity of the PCM during phase transitions, by strengthening the overall sustainability of the thermal storage system [37]. In this study, the thermal efficiency of SiC will be evaluated because several studies confirm that, in phase change material (PCM) thermal storage systems, porous SiC structures offer exceptional durability due to their chemical and mechanical stability during melting-solidification cycles. It maintains the system's integrity, which prevents PCM leakage and greatly reduces the cost of maintenance. SiC is structurally stable, chemically durable, and perhaps most importantly, it undergoes minimal corrosion, especially in the harsh environment of molten salts. In contrast, copper (Cu) and aluminum (Al) oxidise and corrode rapidly, requiring protective coating or an inert atmosphere for an expensive installation and high ongoing maintenance. [38–41]. As well as, SiC has been studied under elevated temperature conditions by several studies, demonstrating that it retains excellent chemical and structural stability even in the presence of aggressive molten salts used in thermal storage systems. The thermodynamic stability of SiC at high temperatures reduces periodic maintenance requirements, extends system life, and improves performance reliability, which contributes to lower overall operating costs over the entire life cycle [42]. Thus, the use of SiC in high temperature applications, especially above 700 °C, has demonstrated its chemical compatibility and thermal stability, which are essential to ensure long-term durability [43]. Many industries have already exploited porous SiC in demanding applications, including water filtration, porous burners, honeycomb diesel particulate filters, hot gas filters, and molten metal filters [44, 45]. Plus separation membranes, acoustic and thermal insulation, high-temperature structural materials, furnace supports, thermoelectric energy conversion, and composite reinforcement [46, 47]. This durability is crucial for PCM composites subjected to repeated thermal cycles [48]. Finally, based on these reasons, the study will focus on optimizing the structure of metal foam (SiC), examining the effect of porosity (85%, 91%, and 97%) and pore density (5, 10, and 20 PPI) on the thermal performance of the PV system in terms of plate temperature, liquid fraction, and PV electrical efficiency. The main objective of this work is to design a passive cooling system for photovoltaic (PV) panels that is both efficient and economically viable. To achieve this, we seek to minimize the costs of the materials used while ensuring optimal efficiency. To this end, we evaluated different combinations of PCM and metal foam (MF). This efficiency improvement not only increases electricity production but also reduces CO_2 emissions, contributing to a more sustainable energy transition. Our approach will help determine the best PCM/MF combination to improve photovoltaic performance while optimizing costs and providing guidance for practical applications to ensure optimal profitability and a rapid return on investment.

2. Mathematical model and method

2.1 Physical model

The configuration comprises two congruent aluminum plates positioned on the lateral aspects of a rectangular cavity that is either filled with phase change material (PCM) or supplemented with foam. To help model the photovoltaic (PV) panel, an aluminum plate is positioned on the left side of the cavity to represent the PV panel, which receives a steady solar radiation intensity of 750 (W/m^2K) and is surrounded by air that has a natural convection coefficient of $(h_1 = 12.5W/m^2K)$. This simplification has been successfully tested in various research [1, 4, 7], leading to reasonable results compared to the PV panel direct modeling. The system's temperature is lowered by dissipating heat to the surrounding air using the right plate $(h_2 = 7.5W/m^2.K)$. The system is adiabatic on both its upper and lower sides. The plates have measurements of $132 \times 4.5\ mm^2$, and those of the cavity are $132 \times 49\ mm^2$, as shown in Fig. 1. The paraffin-based PCMs employed in this study are RT25, RT35, and RT44, which have melting points of 26.6 °C, 35 °C, and 44 °C, respectively. We chose paraffins because of their unique properties, including good chemical and thermal stability, high latent heat, a phase change temperature range suitable for photovoltaic panel cooling systems, and low cost [49, 50]. Table 1 summarizes the thermophysical characteristics of PCMs, aluminum, copper, and silicon carbide foams [49, 51, 52]. The system is numerically modeled to first investigate the effectiveness of various types of paraffins (RT25, RT35, and RT44) with the aim of determining the optimal type of PCM for PV cooling performance. To improve the PCM's low thermal conductivity, various types of foam (copper foam, aluminum foam, and silicon carbide foam) are incorporated into RT25 to evaluate their impact on overall system performance in terms of electrical efficiency and foam cost. Finally, the impacts of varying foam porosity (85%, 91%, and 97%) and pore density (5, 10, and 20 PPI) in the SiC foam/RT25 composite are thoroughly investigated.

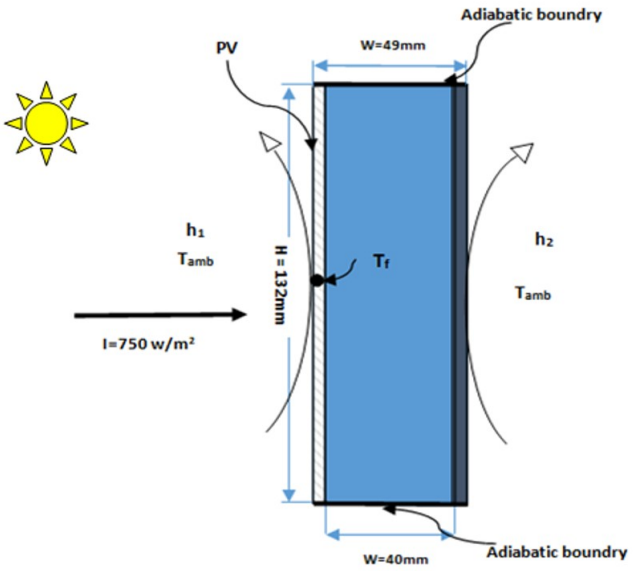

Figure 1. Depicts a two-dimensional schematic representation of the studied configuration.

Table 1. Properties of PCMs and MFs in terms of thermophysics [49, 51, 52].

Material	ρ (kg/m^3)	K $(W/m/K)$	C_p $(J/kg/K)$	T_m C °	L kJ/kg
RT25 (s/l)	785/749	0.19/0.18	1800/2400	26.6	232
RT35 (s/l)	880	0.2	2000	34/36	240
RT44 (s/l)	800	0.2	2000	41/44	250
Aluminum	3600	211	765	—	—
Cu MF	8954	400	383	—	—
Al MF	2719	202.4	871	—	—
SiC MF	3100	118	1150	—	—

2.2 Mathematical formulation

2.2.1 Numerical approach

Because of the complexity of the structure of foam/PCM composites, the above-mentioned configuration implies complicated thermal transport processes. To reduce this complexity in terms of tracing the foam structures and the high computing cost, we used the volume-averaging approach to transform the transport equations from the pore scale to the macroscopic scale over a representative elementary volume (REV). Additionally, this method is based on the ideas of local thermal equilibrium (LTE) and local thermal non-equilibrium (LTNE). The current study used the LTE model, which is based on the idea that there is local thermal equilibrium between the foam and the phase change material (PCM). Using this method is quite simple, leads to good results, and is often mentioned in research to address the challenges of liquid flow and heat transfer related to phase changes in foam materials [3]. Additionally, the enthalpy-porosity model suggested by Voller and Prakash is used to model how phase change materials (PCMs) melt.

2.2.2 Governing equations

The foam was modeled as a continuous and homogenous porous medium using the Darcy-Forchheimer-Brinkman (DFBM) model, adding a source term to

explain its existence in the momentum equation. The local thermal equilibrium (LTE) is employed to address the phase change material (PCM) energy equation in the context of foam presence. This choice is supported by the need to improve computing speed while keeping the results accurate, since the LTE framework assumes that the melting fraction (MF) and PCM in each cell are at the same temperature [53]. The equations governing continuity, momentum, and energy are formulated based on the following assumptions.

- The open-cell foams and PCMs, and plates are assumed to be homogeneous and isotropic.
- The liquid PCM is considered 2D, compressible, laminar and Newtonian.
- In the energy equation, the PCM and MF are considered to be in local thermal equilibrium.
- During the phase change process, PCM's volumetric growth is minimal.
- The Boussinesq approximation is a mathematical tool used to model how changes in the density of liquid phase change materials (PCMs) affect their behavior.
- The PV is considered to be an aluminum plate with homogeneous and isotropic properties.

The governing equations may be articulated in the following manner, utilizing the aforementioned assumptions.

Continuity equation, Eq. 1:

$$\frac{\partial u}{\partial x}+v\frac{\partial u}{\partial y}=0 \tag{1}$$

Momentum equation, Eqs. 2, 3, 4, and 5:

$$\frac{\rho_{PCM}}{\varepsilon}\left(\frac{\partial u}{\partial t}+\frac{u}{\varepsilon}\frac{\partial u}{\partial x}+\frac{v}{\varepsilon}\frac{\partial u}{\partial y}\right)=-\frac{\partial p}{\partial x}+\frac{\mu_{PCM}}{\varepsilon}\left(\frac{\partial^2 u}{\partial x^2}+\frac{\partial^2 u}{\partial y^2}\right)+S_u \tag{2}$$

$$S_u=-A_m\frac{(1-f_1)^2}{(f_1^3-0.001)}u-\left(\frac{\mu_{PCM}}{K}u+\frac{C_F}{\sqrt{K}}\,\rho_{PCM}\,u\sqrt{u^2+v^2}\right) \tag{3}$$

$$\frac{\rho_{PCM}}{\varepsilon}\left(\frac{\partial v}{\partial t}+\frac{u}{\varepsilon}\frac{\partial v}{\partial x}+\frac{v}{\varepsilon}\frac{\partial v}{\partial y}\right)=-\frac{\partial p}{\partial x}+\frac{\mu_{PCM}}{\varepsilon}\left(\frac{\partial^2 v}{\partial x^2}+\frac{\partial^2 v}{\partial y^2}\right)+S_v \tag{4}$$

$$S_v=(\rho\beta)_{PCM}\,g\,(T-T_{ref})-A_m\frac{(1-f_1)^2}{(f_1^3-0.001)}v- -\left(\frac{\mu_{PCM}}{K}v+\frac{C_F}{\sqrt{K}}\,\rho_{PCM}\,v\sqrt{u^2+v^2}\right) \tag{5}$$

The dynamic viscosity, density, and thermal expansion coefficient of PCM are denoted by, μ_{PCM} , ρ_{PCM}, and β_{PCM}, respectively. The p represents the pressure, and g is the gravitational acceleration. The A_m refers to the constant associated with the mushy zone, which plays a crucial role in managing the transition behavior between the solid and liquid phases. In the current simulation, the value of A_m is set to $10^5\ kg/m^3s$, which is in accordance with the study reported in [54]. K and C_F represent the permeability and inertia coefficient of porous media.

Energy conservation equation for foam/PCM composite, Eq. 6:

$$\overline{(\rho c_p)}\frac{\partial T}{\partial t}+(\rho c_p)_{PCM}\left(u\frac{\partial T}{\partial x}+v\frac{\partial T}{\partial y}\right)= =k_{eff}\left(\frac{\partial^2 T}{\partial x^2}+\frac{\partial^2 T}{\partial y^2}\right)-\varepsilon\rho_{PCM}\,L_{PCM}\,\frac{\partial f_1}{\partial t} \tag{6}$$

where $\overline{(\rho c_p)}$ represents the volumetric heat capacity of (MF+PCM), which is calculated by Eq. 7.

$$\overline{(\rho c_p)}=[1-\varepsilon]\,(\rho C_p)_{MF}+\rho(\rho C_p)_{PCM} \tag{7}$$

where $((\rho C_p)_{PCM})$ is the volumetric heat capacities of PCM and $((\rho C_p)_{MF})$ for MF, The (L_{PCM}) represents the latent heat of PCM. The effective thermal conductivity (k_{eff}), is calculated as the volume-averaged thermal conductivity of MF and PCM, as follows, Eq. 8:

$$k_{eff}=(1-\varepsilon)\,k_{MF}+\varepsilon\,k_{PCM} \tag{8}$$

where k_{MF} and k_{PCM} are the thermal conductivities of MF and PCM, respectively. The liquid fraction of $PCM(f_l)$ that occurs during the solid-liquid phase transition is calculated as follows, Eq. 9:

$$f_l=\frac{\Delta H_{PCM}}{L_{PCM}}=\begin{pmatrix}0 & if\Rightarrow T<T_s\\ 1 & if\Rightarrow T>T_l\\ \frac{T-T_s}{T_l-T_s} & if\Rightarrow T_s\le T\le T_l\end{pmatrix} \tag{9}$$

where ΔH_{PCM} and L_{PCM} represent the fractional latent-heat and latent heat of PCM, respectively. During the phase change process, ΔH_{PCM} is expressed as follows, Eq. 10:

$$\Delta H_{PCM}=\begin{pmatrix}0 & if\Rightarrow T<T_m\\ f_l L_{PCM} & if\Rightarrow T>T_m\end{pmatrix} \tag{10}$$

where T_m is the melting temperature of PCM. The total enthalpy (H) is defined as the sum of the sensible heat (h) and fractional latent-heat (ΔH_{PCM}) of PCM, as follows, Eq. 11:

$$H=h+\Delta H_{PCM} \tag{11}$$

where h is expressed as follows, Eq. 12:

$$h=h_{ref}+\int_{T_{ref}}^{T}Cp_{PCM} \tag{12}$$

where h_{ref} and T_{ref} are the reference enthalpy and reference temperature, respectively

2.2.3 Parameters of foam

Permeability (K) is a crucial characteristic that connects the pressure gradient to the flow velocity in a laminar flow regime where the gradient is the primary driver. In order to accurately characterize fluid properties in porous media, Calmidi and Mahajan [55] established a correlation that may be used to quantify both permeability and the coefficient of inertia (CF). The following method is essential for comprehending flow phenomena where viscosity and pressure factors predominate Eqs. 13 and 14.

$$K=0.00073\,d_p^2\,(1-\varepsilon)^{-0.224}\left(\frac{d_l}{d_p}\right)^{-1.11} \tag{13}$$

$$C_f=0.00212\,(1-\varepsilon)-0.132\left(\frac{d_l}{d_p}\right)^{-1.63} \tag{14}$$

The MF structure is described using several fundamental parameters, including porosity (ε), characteristic diameter of solid elements (ligaments or cells) (d_l), typical pore diameter or size (d_p), and pore density (ω). Porosity (ε) quantifies the void fraction in the MF, while pore density (ω), expressed in PPI, indicates the number of pores present per unit length. Thus giving an estimate of the distribution and concentration of pores within the material. Finally, (d_l), can be calculated based on (d_p) using the relation proposed by [55], enabling a more precise modeling of the porous structure, Eqs. 15 and 16.

$$d_l=1.18\,d_p\sqrt{\frac{1-\varepsilon}{3\pi}}\left(\frac{1}{1-e^{-(1-\varepsilon)/0.04}}\right) \tag{15}$$

$$d_p=\frac{0.0245\ m}{\omega(PPI)} \tag{16}$$

Cost and performance estimation of PV cooling systems using PCM and PCM+MF.

The electrical efficiency of PV cells is related to the temperature of the PV front surface using the following, Eq. 17.

$$\eta=\eta_o\,[1-\beta_o(T_{pv}-298)] \tag{17}$$

where (β_o) is the temperature coefficient of silicon efficiency, which is taken to be $0.005\ K^{-1}$, and the typical PV cell efficiency at 298 K, η_o, is 17.1% according to the manufacturer's datasheet. Furthermore, the cell temperature is indicated by T_{pv} [34]. The outlet power is determined by Eq. 18.

$$P_{outlet}=\eta\times I\times A_{pv} \tag{18}$$

Where outlet power (P_{outlet}), solar irradiation (I), and surface area of PV cells (A_{pv}) [45]. This section examines the financial benefits of improving PV efficiency through a passive cooling system. This is based on optimizing heat dissipation to stabilize and reduce the PV temperature, through integrating

phase change materials (PCM) and PCM combined with metal foam. These materials allow for more efficient thermal management, thus limiting energy losses and increasing electricity production, which improves the profitability of the installation. To do this, we establish an economic estimate of the costs of the materials added in the cases studied previously, as well as the gains obtained. To maximize these benefits and ensure an optimal return on investment, a rigorous selection of materials is essential. The objective is to find a balance between thermal performance and acquisition cost.
Table 2 presents the costs of the different materials used for cooling PV panels. These costs were calculated considering a thickness of 40 mm applied on the back side of the PV and a surface area of 1 m^2. The unit prices of the materials are based on the values provided by the manufacturers. This comparative analysis aims to identify the most advantageous combination, allowing for minimizing the initial costs while ensuring a sustainable improvement of photovoltaic production. With an electricity tariff set at 0.15 €/kWh [56], the increase in electricity production by PV generates significant annual savings on energy costs, thus reinforcing the economic viability of the proposed cooling system.

Table 2. The cost of the materials used for thermal management reported in this work per m^2 of the studied PV surface, [57, 58].

Item	Rate ($)	Cost $/$m^2$ of PV
Paraffine (RT25)	$1.0/kg$	31.4
Paraffine (RT35)	$1.0/kg$	35.2
Paraffine (RT44)	$1.0/kg$	32
MF(Cu)	$257.25/(1\times1\times0.01m)$	1029
MF(Al)	$202.5/(1\times1\times0.01m)$	900
MF(SiC)	$37.25/(1\times1\times0.01m)$	149

2.2.4 Environmental analysis

Fossil energy sources are known for their negative environmental impact. At the same time, electricity production from sustainable and clean systems, such as photovoltaic (PV) technologies, represents a promising alternative to limit greenhouse gas emissions. In this study, the improvement in the performance of photovoltaic panels was achieved through the integration of a phase change material (PCM) associated with a metal foam, allowing better thermal management and an increase in their efficiency. In order to evaluate the environmental impact of the system studied and demonstrate its advantages compared to conventional energy sources, an analysis was carried out by quantifying the reduction in CO_2 emissions obtained thanks to this optimization. It is estimated that electricity production from fossil thermal power plants generates around 2 kg of CO_2 $(1/kWh)$ [59], and it is even estimated by (IPCC (2006) [60], which reports average emission factors of 0.9 to 1.1 $kg\ CO_2/kWh$ for coal-fired electricity generation in some developing countries. However, considering the average efficiency of thermal power plants (33–35%) as well as transmission and distribution losses, some studies use an approximate value of 2 $kg\ CO_2/kWh$ of final energy consumed in simplified calculations of environmental-economic analyses, in order to more accurately reflect the impact of emissions from primary energy (IEA, 2023) [61]. It is important to note, however, that this value may vary depending on the regional energy mix, being higher in regions with high coal dependence and lower (0.4–0.6 $kg\ CO_2/kWh$) in regions with a significant share of renewable energy or natural gas in their electricity generation [61]. Thus, by integrating PCM and metal foam to improve the efficiency of photovoltaic panels, it becomes possible to reduce greenhouse gas emissions further.

2.3 Initial and boundary conditions

Thus, for the PV/PCM system, the initial temperature $T_{in} = 293.15\ K$ (20 °C) was chosen in consistency with the boundary conditions used in [36], which we followed to ensure consistency and comparability of our results with this study in order to see the improvement made compared to their results. This value is also close to the standard ambient conditions used in experimental studies on photovoltaic systems. The heat transfer coefficients by convection on the front and rear surfaces were estimated to be $h_1 = 12.5\ W/m^2K$ and $h_2 = 7.5\ W/m^2K$, respectively, with solar radiation of 750 W/m^2 applied to the front surface. The upper and lower surfaces are assumed to be adiabatic.

1- The initial conditions as $t = 0 \rightarrow T = T_{ini} = 293.15\ K,\ \ f_l = 0$, [49].
2- Boundary conditions, Eqs. 19 and 20.

$$-\lambda_{Al}\frac{\partial T}{\partial x} \rightarrow at\ Front\ plate = I + h_1(T - T_{amb}) \tag{19}$$

$$-\lambda_{Al}\frac{\partial T}{\partial x} \rightarrow at\ Back\ plate = h_2(T - T_{amb}) \tag{20}$$

The top and bottom walls of the system are considered adiabatic, as described in the Eq. 21.

$$\frac{\partial T}{\partial y} = 0 \tag{21}$$

The contact surfaces between the aluminum plates and the PCM were considered according to energy balance conditions expressed by Eq. 22.

$$\lambda_{Al}\frac{\partial T_{Al}}{\partial x} = \lambda_{PCM}\frac{\partial T_{PCM}}{\partial x} \tag{22}$$

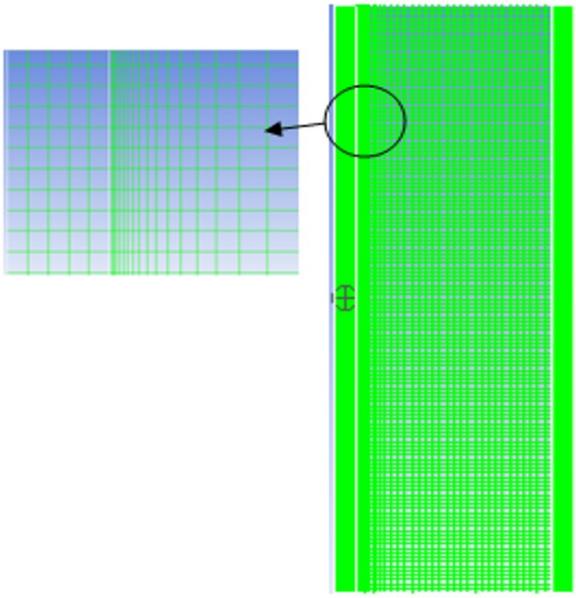

Figure 2. Typical grid distribution (a) and zoom case.

2.4 Numerical method

The commercial CFD program ANSYS-FLUENT 17.0 is used to solve the unstable 2D simulations. The finite volume method (FVM) is used to numerically discretize the conservation equations (continuity, momentum, and energy) with twofold computational precision. We used a melting and solidifying model along with a porous model that assumes local thermal equilibrium (LTE) to study how phase changes happen in PCM and PCM+MF. The enthalpy-porosity-based method put out by Voller and Prakash [62] uses a fixed-grid approach to compute the answer. The ANSYS Fluent software was chosen to address the energy and momentum equations pertinent to the numerical simulation. A second-order upwind scheme was employed to discretize the equations, thereby enhancing the accuracy of the computations. This method allowed for a more precise representation of the thermal and fluid dynamics involved in the phase change processes. By implementing this approach, we aimed to capture the intricate interactions between heat transfer and fluid flow, ultimately leading to a deeper understanding of the performance of phase change materials (PCMs) in various applications. The PRESTO methodology was employed to discretize the pressure, in accordance with the procedures described in [63, 64]. According to [59, 65], the speed-pressure coupling was guaranteed by the PISO algorithm. Under-relaxation coefficients of 0.7, 0.3, 0.9, and 1 for momentum, pressure, liquid fraction, and energy, respectively, were assigned to ensure numerical stability and convergence [66]. The energy and velocity convergence criteria are set at 10^{-7} and 10^{-5}, respectively. Additionally, a 2D planar geometry has been simulated using a mesh of the non-uniform quadratic element type. The mesh-generating program ANSYS GAMBIT 2.4.6 is used to construct these organized quadratic cells. While the rest of the domain uses a uniform grid distribution, the area close to the wall (PV) uses a dense grid distribution. The typical grid distribution across the configuration's computing domain is depicted in the plots of Fig. 2. Grid independence was assessed using three distinct grid sizes: (45×132), (55×132), and (65×132), as shown in Fig. 3a. The findings showed that a mesh with 5940 cells was the most effective option for the existing model, with only a slight improvement shown when the cell count was increased to 8580. To

maximize processing time, this decision was made. Because they have similar features, it is significant to note that the same grid size was likewise applied to all pertinent PV models. A comparison of 0.05, 0.1, and 0.2 seconds, shown in Fig. 3b, showed that the temperature at the front surface of the PV/PCM system was not greatly influenced by the time step chosen. Therefore, we used a 0.2s time step with a grid of 5940 cells for all cases in this investigation. It took about two to three days to finish each case's numerical computations.

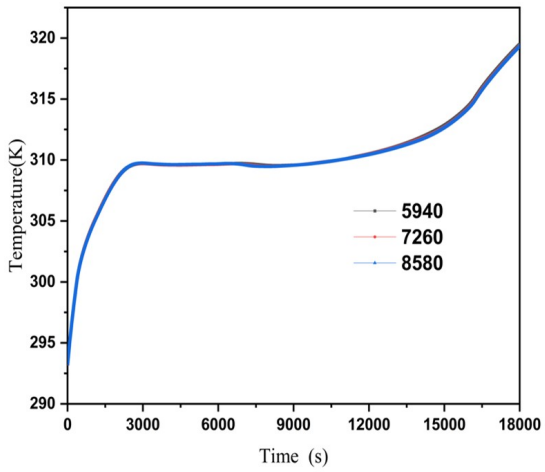

(a) Grid independence analysis

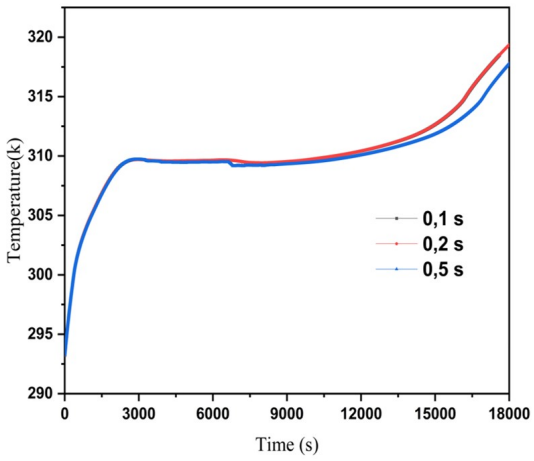

(b) Time step independence analysis

Figure 3. Evolution of Temperature at the front Aluminum plate (T_{pv}).

3. Model validation

In order to evaluate the accuracy of our numerical model, we present in this section three validation cases. The results of our simulations are compared with the numerical and experimental results reported in the literature.

Table 3. The comparison between the numerical results of the present study and the experimental results of Huang et al. [49], and the numerical results of Zhao et al. [67].

	Present study	Experimental	Numerical	Deviation
T (K)	310.11	307.36 [49]	307.62 [49]	0.9%
T (K)	326.93	—	321.77[67]	1.60%

3.1 Experimental and numerical validation for PV-PCM system

We used the temperature (T_{pv}) of the PV/PCM system's front wall for validation. Huang et al. contrasted our numerical results with their experimental and numerical findings. As shown in Table 3, the results from [49] exhibit excellent agreement with those presented in Fig. 4, leading to a maximum relative difference of 0.9% between the experimental results from [49] and the numerical results of this study. The identical PV/PCM system geometry 132 *mm* high by 49 *mm* wide, as well as the same beginning and boundary conditions and material parameters, were used for our validation [49].

3.2 Experimental and numerical validation for $MF + PCM$

The numerical model was reformulated following the conditions adopted in Refs. [67, 68], enabling the reproduction of the scenario described by the original authors. The configuration utilized in References [67, 68] consists of a rectangular cavity measuring $25 \times 200\ mm^2$, which is filled with phase change material (PCM)-saturated copper foam that exhibits a porosity of 0.95 and a pore density of 10 PPI. The lower surface of the cavity is subjected to a uniform heat flux of 1600 W/m^2, while the other surfaces are exposed to natural convection influences (h = 4 W/m^2K). As listed in Table 3 and shown in figure, it was observed that the results related to LTE are in good agreement with those of Zhao et al. [67] and Liu et al. [68], with a maximum absolute deviation in temperature of 5 °C from Zhao's data.

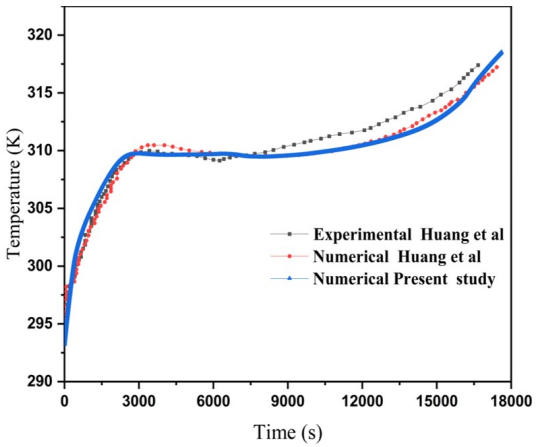

(a) experimental and numerical for the PCM case made by Huang et al. [49].

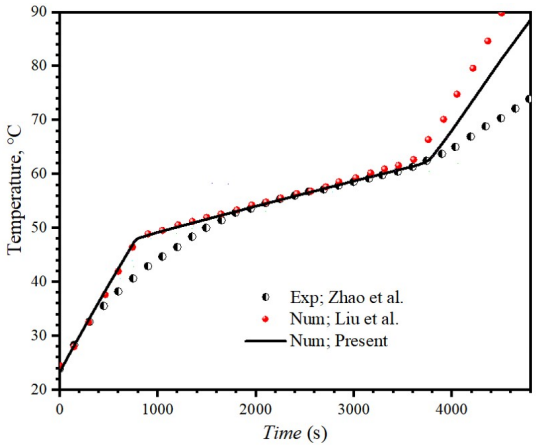

(b) experimental and numerical for the PCM/MF (LTE) case made by Liu et al. and Zhao et al. [67, 68].

Figure 4. Model validation.

4. Results and discussions

In this section, results concerning the influence of the PCM melting point on the cooling performance and electrical efficiency of a solar panel subjected to a continuous irradiance of 750 W/m^2 and an ambient temperature of 20 °C are presented and analyzed. . To achieve this purpose, we investigate three configurations incorporating paraffins RT44, RT35, and RT25, with melting points of approximately 42.5 °C, 35 °C, and 26.6 °C, respectively. They all have the same thickness of 40 *mm*. The objective is to compare the effectiveness of these PCMs to determine which one will provide the best improvement in photovoltaic performance. Next, the effect of the foam material type combined with a suitable PCM will be examined. The choice of the foam material is made taking into account thermal efficiency as well as acquisition cost. We selected three types of foams: copper (Cu), aluminum (Al), and silicon carbide (SiC), all with a porosity of 97% and a pore density of 5 PPI, in order to determine

which combination offers the best compromise between efficiency and cost. We then provide the findings related to the impact of varying the SiC foam's pore density (5, 10, and 20 PPI) at $\varepsilon = 97\%$. We then examine the impact of changing the porosity (85%, 91%, and 97%) of SiC foam with 5 PPI. We present the findings in relation to the melting time of PCM, the liquid fraction, the operating temperature of PV, and its electrical efficiency. These parameters make it possible to evaluate the impact of different configurations. Next, we present an analysis of the electrical performance of PV optimized by the integration of PCM and MF. The objective is to assess the impact of these cooling solutions on the energy efficiency of PV and to analyze the environmental and economic benefits gained compared to a standard PV. First, an economic estimate is carried out to identify the most cost-effective combination of materials by selecting those offering the best compromise between cost and thermal performance. This analysis is based on an evaluation of the costs of the different PCMs used, thus making it possible to choose the least expensive solution while guaranteeing a significant improvement in the efficiency of PV. Then, an estimation of the cost of the different $PV/PCM+MF$ configurations is carried out by integrating several types of metal foams (MF) combined with the selected PCM. Then, we evaluate the increase in electrical energy production obtained thanks to improved PV efficiency. Finally, we quantify the reduction in CO_2 emissions enabled by these improvements.

4.1 Effect of PCM type on PV performance

This section compares and examines the effectiveness of three different types of paraffin (RT44, RT35, and RT25) in enhancing the PV system's performance under identical operating conditions. The time evolution of the PV operating temperature is displayed in Fig. 5a for the reference scenario without PCM and a PV module in combination with RT44, RT35, and RT25. When compared to a standard PV system, it is evident that the PV+PCM cooling system considerably lowers the PV operating temperature. In the case of RT44, the maximum temperature that can be achieved after 60 minutes of operation with 750 W/m^2 of sunshine, an ambient temperature of 20 °C, and 40 mm of three PCM thickness is 50 °C. However, Ref. [36] showed that the temperature of PV can surpass 63 °C with natural cooling. Furthermore, Fig. 5a, which shows the evolution of the PV average temperature as a function of time by contrasting the case of a PV alone with that of a PV associated with different PCMs (RT44, RT35, and RT25), demonstrates that the type of PCM (i.e., melting point) has a significant impact on the thermal regulation of the PV. This indicates that the operating temperature of the PV is comparable to the PCM's average temperature. According to Fig. 5a, the curve for PV alone demonstrates a sharp rise in PV temperature over the first two hours, peaking at 330.15 K. The temperature then steadies, signifying that a thermal equilibrium has been established as a result of natural convection with the outside world. However, the presence of PCM can help us understand why the PCM sensitively absorbs the heat that the PV dissipates during the first time. The PCM then starts to melt as its heat transfer increases. The PCM temperature varies very little during this time. After complete melting, the PV's temperature rises noticeably. These findings indicate that the PCM's melting point has a major impact on the PV's operating temperature. Accordingly, the average PV temperature for RT25, RT35, and RT44 after three hours of operation is 310 K, 315 K, and 323.5 K, respectively. The findings also demonstrate that, under the same conditions used in our study, the maximum temperature of the PV without a cooling system reached 331 K after three hours of operation; our findings indicate that this temperature is lowered by 21 °C for a thickness of 4 cm utilizing RT25. In addition, as compared to PV alone, RT35 and RT44 lower the PV operating temperature by 16 °C and 8.5 °C, respectively. Equation 21 is used to compute the PV's efficiency; it indicates that 298 K is the ideal temperature for the PV. Thereafter, as the PV temperature rises, efficiency falls. The evolution of the photovoltaic (PV) panel's electrical efficiency over time is shown in Fig. 5b. The results show an inverse relationship between the efficiency and the PV's temperature. For RT25, RT35, and RT44, the corresponding PV's electrical efficiency is 16.10%, 15.67%, and 14.99%, respectively. RT25 improves electrical efficiency by 12.42%, whereas RT35 and RT44 improve electrical efficiency by 9.4% and 4.18%, respectively. This graph demonstrates how the low-melting-point PCM improves the PV system's overall performance. Fig. 5c illustrates how the liquid fraction of PCM varies for several PCM types. For the same amount of PCM, it is clear that the liquid percentage of PCM rises as the melting point of PCM falls. The maximum reduction in PV temperature is made achievable by this rise in liquid percentage. Furthermore, it is noted that RT25's liquid percentage is greater than RT35's and RT44's, suggesting that the cooling system employing RT25 absorbs more heat. As a result, the PCM type allowed for the PV to operate at its lowest temperature.

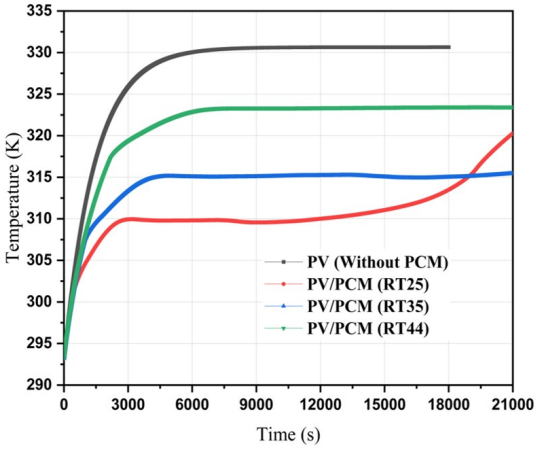

(a) operating temperature (T_{pv}).

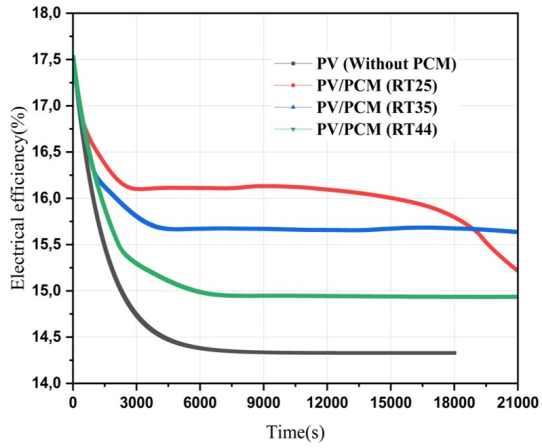

(b) Electrical efficiency (η).

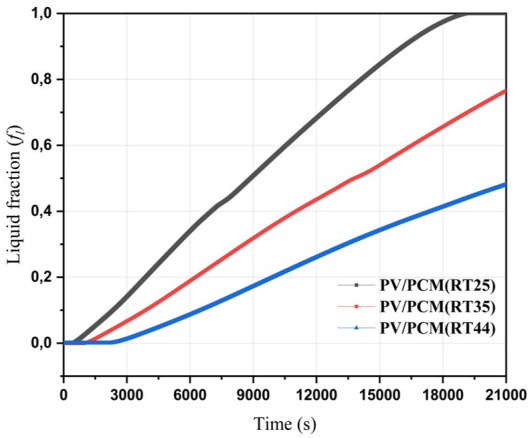

(c) Liquid fraction (f_l).

Figure 5. Effect of MCP type.

4.2 Effect of MF materials on PV performance

To investigate the impact of magnetically functionalized (MF) materials on thermal transfer efficacy and the efficiency of energy conversion, we have selected three distinct foam materials: copper (Cu), aluminum (Al), and silicon carbide (SiC), which are integrated with RT25 due to its superior performance in terms of electrical efficiency. In this section, all selected foams possess a porosity of 97% and exhibit a pore density of 5 PPI (pores per inch), intended for an insulation capacity of 750 W/m^2. The transient fluctuations of the photovoltaic (PV) operating temperature for the Cu, Al, and SiC foam combined with phase change materials (PCM) are illustrated in Fig. 6a. It is distinctly observable that the PV configuration that integrates MF and PCM reveals a

substantial decrease in the PV temperature in comparison to the PV system that solely utilizes PCM. The findings indicate that after a duration of 2 hours of operational activity, the most pronounced temperature reduction is achieved with the RT25 combined with Cu foam, succeeded by RT25 with *Al* foam, and subsequently RT25 with SiC foam, in that order. The RT25+Cu foam allows a decrease in T_{pv} of 27 °C compared to the common PV and 6 °C compared to PV+PCM alone, but this is a slight difference in T_{PV} for three varieties of foam. Additionally, the lower T_{pv} is achieved with *Cu* foam due to its high thermal conductivity. Figure 6a also illustrates that in all three $PV/PCM + foam$ configurations, the PV operating temperature remains almost the same during operation.

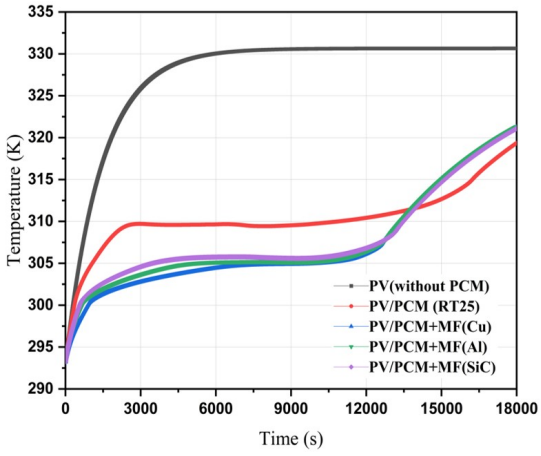

(a) Working temperature (T_{pv}).

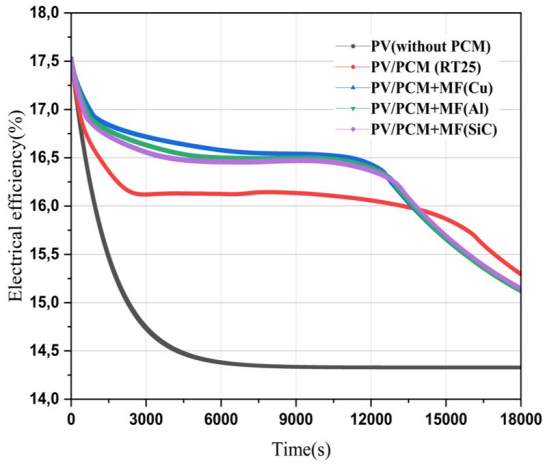

(b) Electrical efficiency (η).

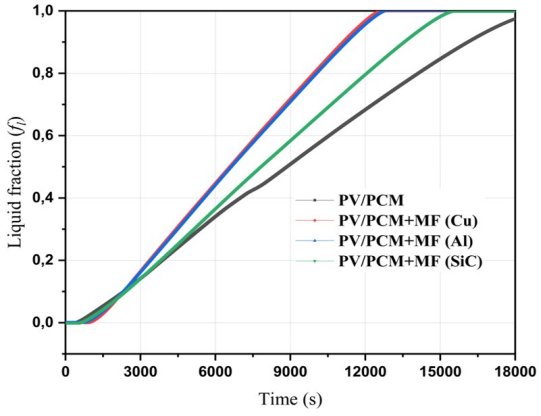

(c) Liquid fraction (f_l).

Figure 6. Effect of different MF.

However, at 4500 s, a notable difference appears where the PV temperature reaches 303 *K* with *Cu* foam, 304 *K* with *Al* foam, and 305 *K* with SiC foam. This reduction in T_{PV} is due to uniform heat transfer from the PV front plate to the back plate. The conjugated heat transfer shows that a photovoltaic panel integrating an MF+PCM offers superior cooling performance. This type of design achieves more efficient cooling than a photovoltaic panel containing only PCM. A comparative analysis of different MF materials reveals that copper (*Cu*) combined with PCM allows the greatest temperature reduction of PV compared to aluminum (*Al*) and silicon carbide (SiC). This increased performance of copper is explained by its higher thermal conductivity than aluminum and silicon carbide. A similar trend is observed for electrical efficiency. Fig. 6b shows that the combination of MF with PCM results in a notable improvement in PV efficiency.

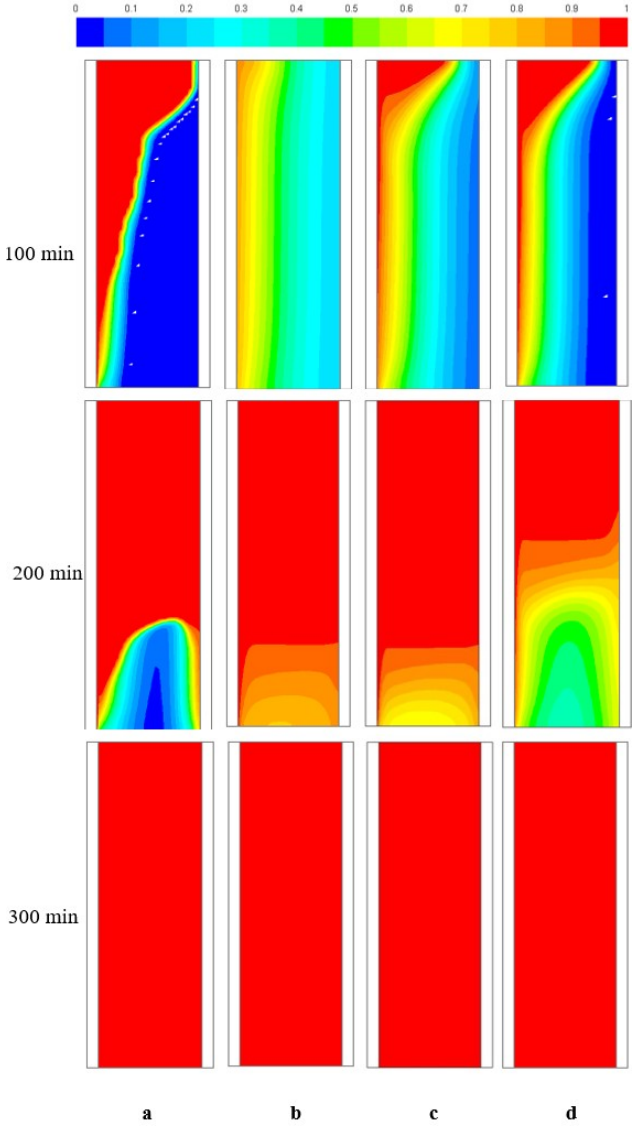

Figure 7. Variation of the liquid fraction at various time intervals of 100, 200, 300 minutes for (a) PCM, (b) MFPCM (Cu),(c)MFPCM (Al) and (d) MFPCM (SiC) cases.

Indeed, this configuration results in an efficiency increase of 16.18% compared to standard PV and 12% compared to PCM alone. After 12000 s, a decrease in efficiency is observed in the PCM+MF cases, which can be explained by the fact that after the complete melting of the PCM, its temperature increases, which affects the PV temperature and thus leads to a decrease in efficiency. Comparing the three types of MF, a minimal difference is observed at 4500 s of operation: the PV efficiency reaches 16.18%, 15.5%, and 15.14% for the MF+PCM Cu, Al, and SiC, respectively. The evolution of the liquid fraction (f_l) for PV/PCM case and the three cases of PV/PCM+MF is presented in Fig. 6c. It shows us that the t_{melt} of PCM decreases with the integration of

MF+PCM, where, such as the reduction of t_{melt} is 34.1%, 33%, and 18.75% for the Cu, Al, and SiC MF+PCM cases compared to the pure PCM case. The evolution of the liquid fraction (f_l) is illustrated by contours at different times (100, 200, and 300 minutes) in Fig. 7. It is clearly illustrated that the addition of MF to PCM significantly modifies the fusion process. We also note that rapid and uniform melting is obtained in the MF+PCM cases, in particular with Cu MF+PCM. The contour figure shows us that the solid-liquid interfacial zones (respectively in blue and red), where heat transfer occurs, are visible at the start of the process, which explains the influence of gravity and buoyancy. Figure 7 reveals that over time, the solid-liquid interface fades and homogeneous melting occurs for PV/PCM+MF, thanks to the combination of natural convection and conduction. At 200 minutes, it is found that the PCM is completely melted in the case of MF+PCM, while a portion of solid PCM remains in the case of PCM alone, which demonstrates that the integration of MF with PCM improves the heat transfer performance and the melting process.

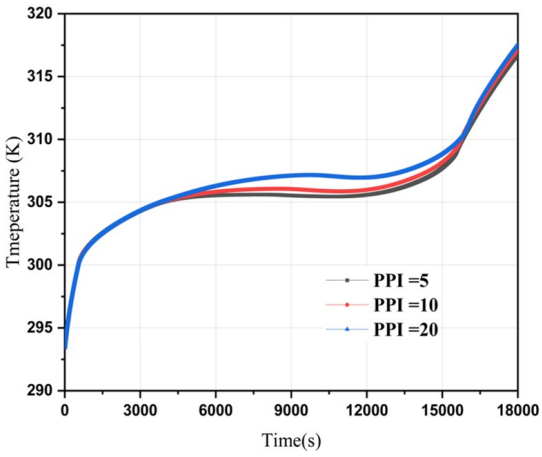

(a) Temperature at the front surface of the Aluminum plate (T_F).

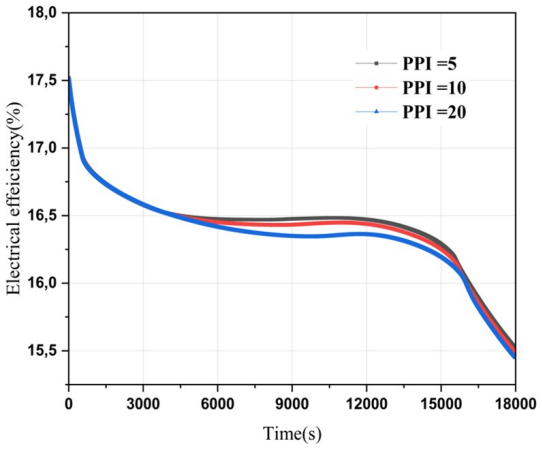

(b) Electrical efficiency (η) variation.

Figure 8. Effect of different PPI.

4.3 Effect of pore density on PV performance

The number of pores per inch in MF is known as pore density. A high pore density indicates that the MF contains a lot of tiny pores. The PV/PCM (RT25+MF(SiC)) system's temperature evolution is displayed in Fig. 8a for varying pore densities (5, 10, and 20 PPI) with a porosity of 97% and an incident flux of 750 W/m^2. The impact of different pore densities on the PV's cooling efficiency is shown in Fig. 8a. The findings show that while the temperature increases marginally when the pore density rises from 5 to 10 PPI, the temperature increases significantly when the PPI rises from 10 to 20. This outcome can be explained by the fact that when the PPI rises above 10 PPI, the impact of natural convection diminishes. This indicates that the PCM takes more time to melt for the case with 20 PPI while the case of 5 PPI shows a lower temperature of the PV a lower pore density, heat is distributed more slowly through the PCM, which prolongs the melting time. Therefore, a system with a lower pore density will take longer to melt the PCM, which helps in better cooling of the photovoltaic panel. The results show that as the pore density increases from 5 to 10 PPI, the PCM temperature increases slightly during the melting process. As the PPI increases from 10 to 20, the PV plate temperature increases. The lower PV temperature implies that the PCM extracts a lot of heat by natural convection due to the large pore size for 5 PPI. On the other hand, as the pore density exceeds a certain value of 10 PPI, the PV temperature increases because less heat is extracted by the PCM, which explains the positive role of the low PPI value. The efficiency of the photovoltaic (PV) system is inversely proportional to the temperature of the panel. The lower temperature of PV results in better energy conversion efficiency. In the PV/PCM+MF system, the pore density influences the cooling efficiency of PV. Fig. 8b shows that for a lower pore density of 5 PPI, the efficiency remains relatively stable for longer. This is because a lower pore density slows down the distribution of heat through the PCM, thereby prolonging the melting time of the phase change material (PCM). As a result, the temperature of the PV remains lower for a longer period, allowing efficiency to remain high. The results obtained show that the efficiency of the photovoltaic (PV) system varies slightly depending on the pore density. For pore densities of 5, 10, and 20 PPI, the average efficiency over a period of 18,000 s is 16.42%, 16.4%, and 16.36%, respectively.

4.4 Effect of porosity on PV performance

The average front surface temperature evolution of the PV for the SiC MF+PCM(RT25) system and electrical efficiency (η) as a function of time are shown in Fig. 9. In this study, the pore density is fixed at 5 PPI, and the irradiance remains constant 750 W/m^2 under different values of porosity (0.97, 0.91, and 0.85). The effects of varying the porosity on the PV working temperature (T_w) and electrical efficiency (η) are illustrated in Fig. 9.

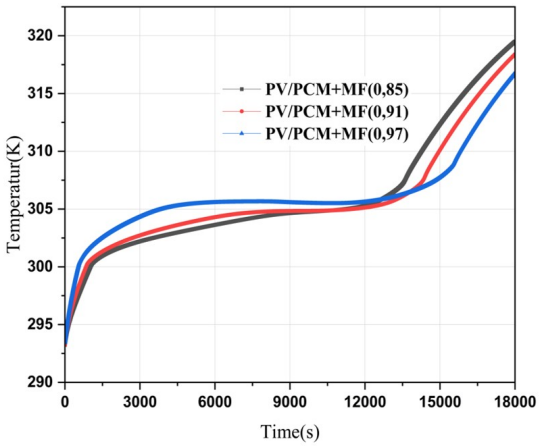

(a) Temperature at the front surface of the Aluminum plate (T_F).

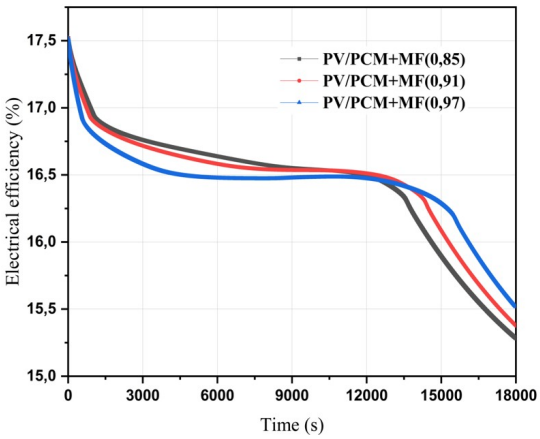

(b) Electrical efficiency (η) variation.

Figure 9. Effect of different porosities.

Initially, the system is at ambient temperature of 293 K then a rapid increase in temperature is observed for all three configurations, indicating the absorption of solar energy and the system temperature rise, after 3000 s; the temperature remains relatively stable, indicating that the PCM absorbs some of the heat and

prevents a rapid rise in the PV temperature, From 12,000 s, a new temperature rise is observed for all configurations, which may be due to the exhaustion of the thermal storage capacity of the PCM. The PV/PCM+MF configuration (0.97) shows a slightly higher temperature than the other configurations at the beginning, but it becomes the lowest at the end of the cycle, suggesting more efficient heat dissipation in the long term. The high porosity configuration (97%) offers a better cooling capacity, especially in the long term, because it can contain more phase change material. This allows for more efficient thermal regulation of the system, resulting in a reduction in the temperature of the photovoltaic panel and an improvement in electrical efficiency. The curve corresponding to lower porosity shows a faster increase in temperature and a more marked drop in efficiency. Fig. 9b shows that the electrical efficiency of the PV panel is significantly influenced by the porosity of SiC MF. Higher porosity allows for better thermal management, which maintains a lower temperature and, therefore, improves the electrical efficiency of the panel.

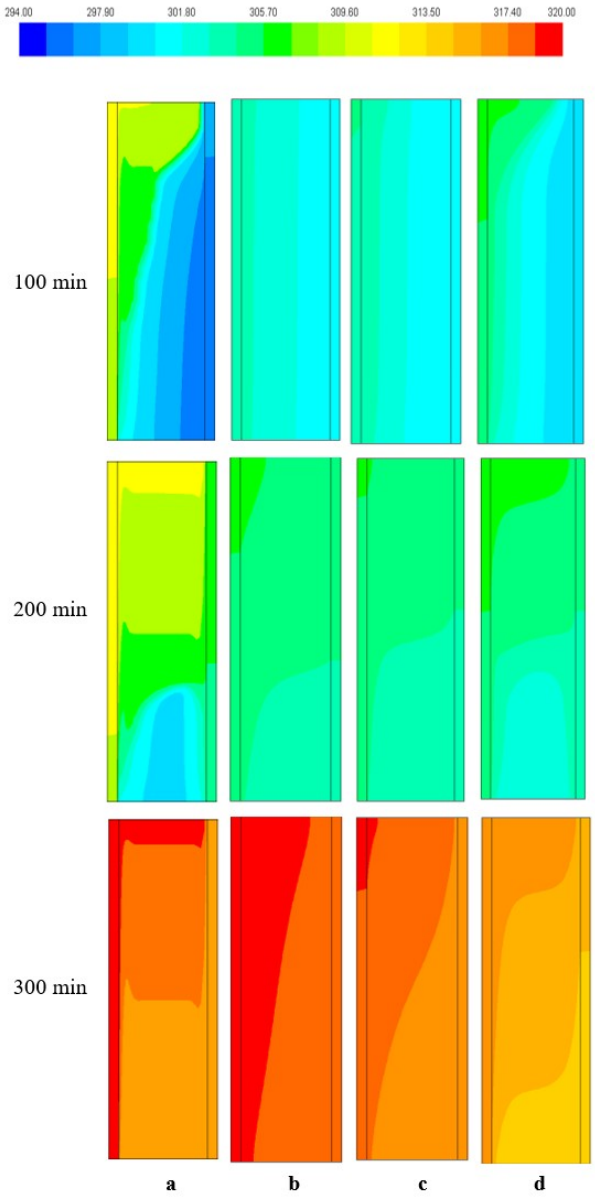

Figure 10**.** Variation of isotherms contours at various time intervals of 100, 200 and 300 mins ;(a) PCM (RT25) and for different porosities of MF(SiC)+PCM(RT25) ;(b)97%, (c) 91%, (d) and 85%.

As the porosity decreases, the PCM melting time is reduced, which accelerates the temperature increase of the PV panel, thereby leading to a decrease in electrical efficiency. The results show that porosity reduction has a very slight influence on the average electrical efficiency of the system over a period of 18,000 s, with values of 16.43%, 16.48%, and 16.52% for porosities of 0.85, 0.91, and 0.97, respectively. In conclusion, a metal foam with higher porosity promotes better electrical efficiency of the photovoltaic panel by reducing its operating temperature. Figure 10 shows the temperature contours within the PCM combined with metal foam (MF/PCM) for three different porosity levels (85%, 91% and 97%) at different times (50 min, 100 min, 150 min, 200 min, 250 min, and 300 min). Initially (50 min), the temperature is low and relatively homogeneous, indicating the beginning of heat absorption. Over time, the temperature gradually increases, reflecting progressive heat storage in the PCM. Figure 10 eloquently illustrates the significant impact of integrating metal foam (MF) within a phase change material (PCM) on the temperature distribution and kinetics in an MF/PCMM system. The comparative study for three levels of metal foam porosity (85%, 91%, and 97%) at key time points (100 min, 200 min, and 300 min) reveals distinct and informative thermal dynamics, implicitly compared to a PV/PCM system without metal foam. Initially, at 100 minutes, the homogeneous temperature observed in all MF/PCM configurations signals an early phase of uniform thermal absorption throughout the PCM volume. However, the temporal evolution of the temperature contours highlights the crucial role of the metal foam in enhancing heat transfer within the PCM. The key observation lies in the difference in thermal behaviour as a function of porosity. The MF/PCM configuration with low porosity (85%) exhibits a faster temperature rise and greater heat accumulation. Such behaviour suggests a higher effective thermal conductivity due to the higher metal volume fraction, thus accelerating the thermal loading process of the PCM. However, this rapidity is potentially accompanied by earlier thermal saturation of the PCM. Conversely, the high porosity configuration (97%) demonstrates a remarkably more uniform thermal distribution throughout the PCM, maintaining a slightly lower temperature after 300 minutes compared to the other configurations. This behaviour indicates better overall thermal management, where heat is distributed more efficiently within the PCM, thus delaying excessive temperature rise. Although the amount of metal foam is reduced at high porosity, the porous structure promotes better heat penetration and diffusion within the PCM matrix. It is worth noting the implication of the absence of metal foam (mentioned as exhibiting clear isotherms). This observation suggests an intrinsically lower thermal conductivity of PCM alone, leading to steeper temperature gradients and less thermal homogeneity. The introduction of metal foam, regardless of its porosity, therefore significantly improves temperature uniformity. From an economic perspective, the argument for high porosity is compelling. Although higher porosity implies a lower amount of metal material (and therefore potentially lower material cost), it appears to offer a beneficial trade-off in terms of improved thermal management. Optimizing thermal performance with a reduced amount of material is a key factor in improving the overall profitability of photovoltaic systems integrating thermal storage.

4.5 Economic analysis

Figure 11 compares three photovoltaic (PV) configurations incorporating phase change material (PCM) and metal foam (MF) in terms of cost ($) and electrical efficiency (%). The results show that the PV/PCM+MF (Cu) configuration is the most expensive, while the PV/PCM+MF (SiC) solution is the most economical, with a significantly lower cost. However, despite these cost differences, the electrical efficiency of the three configurations remains very close, with a minimal gap between them. Thus, the configuration using silicon carbide (SiC) appears to be the optimal choice, as it allows for significant cost reductions while maintaining an electrical efficiency similar to that of copper (Cu). This approach offers a good compromise between performance and cost-effectiveness, making it particularly advantageous for large-scale applications. Therefore the use of porous SiC structures in PCM systems not only ensures high thermal efficiency, but also guarantees increased durability and reliability of thermal storage systems operating under severe thermal cycling conditions. Although the initial cost of SiC materials is generally lower than that of copper (Cu) and aluminum (Al), this economic advantage is reinforced by significantly reduced maintenance costs, replacement, and protective atmosphere requirements, as well as improved long-term thermal efficiency due to resistance to repeated thermal cycling without structural degradation. Therefore, taking into account the total cost of ownership, including installation and maintenance over the entire life cycle, porous SiC structures represent an economically sustainable and technically robust option for phase change material (PCM) thermal storage systems. Considering a photovoltaic (PV) module benefiting from 5 hours (18000s) of maximum sunshine per day, under a solar irradiation of about 750 W/m^2, the results show that the average efficiency of PV is 14.58%, so it can produce about 110 W/m^2. This allows a standard PV (without thermal management materials) to generate about 200 kWh per year. The integration of a phase change material (PCM) improves the efficiency of PV. The addition of metal foam to the PV/PCM system allows to achieve better

improvement. These improvements translate into an increase in the electrical energy produced each year, a reduction in costs thanks to the annual savings made, and a decrease in CO_2 emissions compared to fossil energy sources. Table 4 compares different configurations of photovoltaic (PV) panels integrating phase change materials (PCM) alone and in combination with metal foams (MF). It highlights the positive impact of the integration of PCM and MF on PV efficiency, with a maximum improvement achieved by the PV/PCM (RT25) + MF (Cu) configuration, which shows an efficiency increase of 12%. This improvement translates into an additional electrical energy production of 24 $kWh/m^2/year$, generating a maximum annual saving of \$3.6/m^2. Furthermore, the thermal optimization of the system contributes to a significant reduction in CO_2 emissions, with a decrease of up to $48kg/m^2/year$ for this configuration.

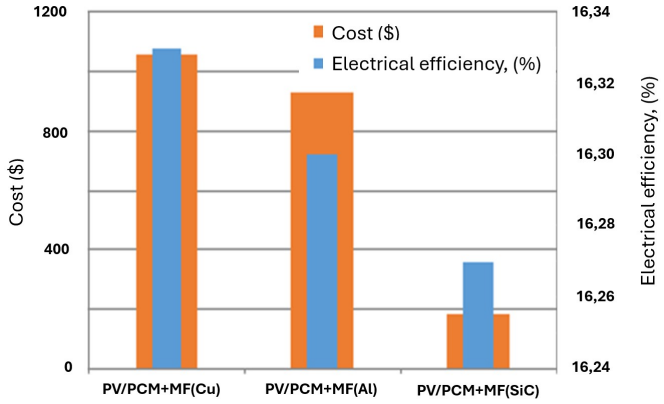

Figure 11**.** Comparison of cost and electrical efficiency of PV/PCM+MF configurations with different metal foams (Cu, Al, SiC).

Table 4**.** Impact of PCM and metal foam integration on efficiency, energy production, annual savings, and CO_2 emission reduction of photovoltaic panels.

	Improved η rate (%)	P_{outlet} added ($KWh/m^2/year$)	annual savings (\$)	CO_2 avoided ($kg/m^2/year$)
PV+RT25+Cu foam	12.0	24	3.6	48.0
PV+RT25+Al foam	11.7	23.0	3.45	46.0
PV+RT25+ SiC foam	11.6	22.6	3.4	45.2

5. Conclusion

The integration of a phase change material (PCM) in a photovoltaic panel allows a significant reduction in its operating temperature, thus improving its electrical efficiency. The addition of a metal foam (MF) further optimizes this thermal management by facilitating heat dissipation. Among the PCMs studied (RT25, RT35, and RT44), RT25 proves to be the most thermally efficient, while having a similar cost to the others, which makes it the optimal choice for cooling PV. Concerning metal foams (Cu, Al, and SiC), although their thermal performances are close, SiC stands out as the most economical solution due to its significantly lower cost. Thus, the optimal combination for better thermal management and reduced cost is the use of PCM RT25 with SiC metal foam. This improvement contributes to an increase in electricity production, generates annual savings, and significantly reduces CO^2 emissions, thus participating in a more sustainable and efficient energy transition. Therefore, the use of porous SiC structures in PCM systems represents both a technically robust and economically sustainable solution for PCM-based thermal storage applications.

Authors' contribution

All authors contributed equally to the preparation of this article.

Declaration of competing interest

The authors declare no conflicts of interest.

Funding source

This study didn't receive any specific funds.

Data availability

The data that support the findings of this study are available from the corresponding author upon reasonable request.

REFERENCES

[1] A. K. Hamzat, A. Z. Sahin, M. I. Omisanya, and L. M. Alhems, "Advances in pv and pvt cooling technologies: A review," *Sustain. Energy Technol. Assess.*, vol. 47, p. 101360, 2021. [Online]. Available: https://doi.org/10.1016/j.seta.2021.101360

[2] Y. Sheikh, M. Jasim, M. Qasim, A. Qaisieh, M. O. Hamdan, and F. Abed, "Enhancing pv solar panel efficiency through integration with a passive multi-layered pcms cooling system: A numerical study," *Int. J. Thermofluid*, vol. 23, p. 100748, 2024. [Online]. Available: https://doi.org/10.1016/j.ijft.2024.100748

[3] M. Y. Othman, A. Ibrahim, G. L. Jin, M. H. Ruslan, and K. Sopian, "Photovoltaic-thermal (pv/t) technology – the future energy technology," *Renew. Energy*, vol. 49, no. 2, p. 171–174, 2013. [Online]. Available: https://doi.org/10.1016/j.renene.2012.01.038

[4] V. Perraki and P. Kounavis, "Effect of temperature and radiation on the parameters of photovoltaic modules," *J. Renew. Sustain. Energy*, vol. 8, no. 1, p. 013102, 2016. [Online]. Available: https://doi.org/10.1063/1.4939561

[5] M. Firoozzadeh, A. Shiravi, and M. Shafiee, "An experimental study on cooling the photovoltaic modules by fins to improve power generation: Economic assessment," *Iranica. J. Energy Environ.*, vol. 10, no. 2, pp. 80–84, 2019. [Online]. Available: https://doi.org/10.5829/IJEE.2019.10.02.02

[6] F. Grubišić-Čabo, S. Nižetić, D. Čoko, I. M. Kragić, and A. Papadopoulos, "Experimental investigation of the passive cooled free-standing photovoltaic panel with fixed aluminum fins on the backside surface," *J. Clean. Prod.*, vol. 176, p. 119–129, 2018. [Online]. Available: https://doi.org/10.1016/j.jclepro.2017.12.149

[7] T. kunihide, "Solaire energy converter using a solaire cell in a shallow liquid-gel layer', united states patent, us 7,244888 b1,," no. 1, 2007.

[8] L. Zhu, R. F. Boehm, Y. Wang, C. Halford, and Y. Sun, "Water immersion cooling of pv cells in a high concentration system," *solar Energy Mater. Sol. Cells*, vol. 95, no. 2, p. 538–545, 2011. [Online]. Available: https://doi.org/10.1016/j.solmat.2010.08.037

[9] S.-Y. Wu, Q.-L. Zhang, L. Xiao, and F.-H. Guo, "A heat pipe photovoltaic/thermal (pv/t) hybrid system and its performance evaluation," *Energy and Buildings*, vol. 43, no. 12, p. 3558–3567, 2011. [Online]. Available: https://doi.org/10.1016/j.enbuild.2011.09.017

[10] H. M. S. Bahaidarah, A. A. B. Baloch, and P. Gandhidasan, "Uniform cooling of photovoltaic panels: A review," *Renew. Sustain. Energy Rev.*, vol. 57, p. 1520–1544, 2016. [Online]. Available: https://doi.org/10.1016/j.rser.2015.12.064

[11] L. Tan, A. Date, G. Fernandes, B. Singh, and S. Ganguly, "Efficiency gains of photovoltaic system using latent heat thermal energy storage," *Energy Procedia*, vol. 110, p. 83–88, 2017. [Online]. Available: https://doi.org/10.1016/j.egypro.2017.03.110

[12] V. J. Reddy, M. F. Ghazali, and S. Kumarasamy, "Innovations in phase change materials for diverse industrial applications: A comprehensive review," *Results Chemistry.*, vol. 8, p. 101552, 2024. [Online]. Available: https://doi.org/10.1016/j.rechem.2024.101552

[13] M. Ismail, W. K. Zahra, S. Ookawara, and H. Hassan, "Boosting the air conditioning unit performance using phase change material: Impact of system configuration," *J. Energy Storage*, vol. 56, no. PartA, p. 105864, 2022. [Online]. Available: https://doi.org/10.1016/j.est.2022.105864

[14] A. S. Soliman, S. Zhu, L. Xu, J. Dong, and P. Cheng, "Melting enhancement of nano-phase change material in cylindrical enclosure using convex/concave dimples: Numerical simulation with experimental validation," *J. Energy Storage*, vol. 44, no. part B, p. 103470, 2021. [Online]. Available: https://doi.org/10.1016/j.est.2021.103470

[15] S. A. Nada and D. H. El-Nagar, "Possibility of using pcms in temperature control and performance enhancements of free stand and building integrated pv modules," *Renew. Energy*, vol. 127, p. 630–641, 2018. [Online]. Available: http://doi.org/10.1016/j.renene.2018.05.010

[16] X. Yang, L. Sun, Y. Yuan, X. Zhao, and X. Cao, "Experimental investigation on performance comparison of pv/t-pcm system and pv/t system," *Renew. Energy*, vol. 119, no. 2, p. 152–159, 2018. [Online]. Available: https://doi.org/10.1016/j.renene.2017.11.094

[17] M. B. Elsheniti, S. Zaheer, O. Zeitoun, H. Alshehri, A. AlRabiah, and Z. Almutairi, "Experimental evaluation of a solar low-concentration photovoltaic/thermal system combined with a phase-change material cooling technique," *Appl. Sci*, vol. 13, no. 1, p. 25, 2022. [Online]. Available: https://doi.org/10.3390/app13010025

[18] P. B, V. A. A, G. P, A. M. M. S. A, and A. T, "Solar photovoltaic cooling using paraffin phase change material: Comprehensive assessment," *Renewable and Sustainable Energy Reviews*, vol. 197, p. 114372, 2024. [Online]. Available: https://doi.org/10.1016/j.rser.2024.114372

[19] S. Khanna, K. S. Reddy, and T. K. Mallick, "Performance analysis of tilted photovoltaic system integrated with phase change material under varying operating conditions," *Energy*, vol. 133, p. 887–899, 2017. [Online]. Available: https://doi.org/10.1016/j.energy.2017.05.150

[20] O. K. A. M. M. Awad and O. M. Ali, "Performance of bi-fluid pv/thermal collector integrated with phase change material: Experimental assessment," *Sol. Energy*, vol. 235, p. 50–61, 2022. [Online]. Available: https://doi.org/10.1016/j.solener.2022.02.031

[21] H. Chen, J. Zhang, M. Shen, H. Fang, and Y. Ma, "Comprehensive numerical modeling of intermittent flow cooling with enhanced photovoltaic efficiency in pvt/npcm systems," *Case Stud. Therm. Eng.*, vol. 58, p. 104420, 2024. [Online]. Available: https://doi.org/10.1016/j.csite.2024.104420

[22] W. W. N. Li, L. Che, Y. Fan, H. Liu, J. Ji, and B. Yu, "A continuous 24-hour power generated pv-teg-pcm hybrid system enabled by solar diurnal photovoltaic/thermal conversion and nocturnal sky radiative cooling," *Energy Convers. Manag.*, vol. 321, p. 119086, 2024. [Online]. Available: https://doi.org/10.1016/j.enconman.2024.119086

[23] S. Lv, J. Yang, J. Ren, B. Zhang, Y. Lai, and Z. Chang, "Research and numerical analysis on performance optimization of photovoltaic-thermoelectric system incorporated with phase change materials," *Energy*, vol. 263, p. 125850, 2023. [Online]. Available: https://doi.org/10.1016/j.energy.2022.125850

[24] T. Ibrahim, M. E. Hazar, F. Hachem, and M. Khaled, "A comprehensive experimental study of cooling photovoltaic panels using phase change materials under free and forced convection – experiments and transient analysis," *J. Energy Storage*, vol. 81, p. 110511, 2024. [Online]. Available: https://doi.org/10.1016/j.est.2024.110511

[25] M. Firoozzadeh and A. H. Shiravi, "Simultaneous use of porous medium and phase change material as coolant of photovoltaic modules; thermodynamic analysis," *J.Energy Storage*, vol. 54, p. 105276, 2022. [Online]. Available: https://doi.org/10.1016/j.est.2022.105276

[26] A. R. Abdulmunem, P. M. Samin, H. A. Rahman, H. A. Hussien, and I. I. Mazali, "Enhancing pv cell's electrical efficiency using phase change material with copper foam matrix and multi-walled carbon nanotubes as passive cooling method," *Renew. Energy*, vol. 160, no. 4, p. 663–675, 2020. [Online]. Available: https://doi.org/10.1016/j.renene.2020.07.037

[27] F. Hachem, B. Abdulhay, M. Ramadan, H. E. Hage, M. G. E. Rab, and M. Khaled, "Improving the performance of photovoltaic cells using pure and combined phase change materials – experiments and transient energy balance," *Renew. Energy*, vol. 107, no. 6, p. 567–575, 2017. [Online]. Available: https://doi.org/10.1016/j.renene.2017.02.032

[28] M. Errebii, A. Mourid, M. E. Alami, and Y. Yao, "Analysis of the impact of metal foam with phase change material on solar photovoltaic thermal system efficiency," *J. Energy Storage,*, vol. 98, no. part A, p. 113064, 2024. [Online]. Available: https://doi.org/10.1016/j.est.2024.113064

[29] Errebii, A. Mourid, M. E. Alami, and Y. Yao, "Evaluation and optimization of thermal exchange performance for a metal foam/phase change material composite integrated into a heat sink," *J. Energy Storage*, vol. 99, no. Part A, p. 113211, 2024. [Online]. Available: https://doi.org/10.1016/j.est.2024.113211

[30] P. Rathore and S. Shukla, "Enhanced thermophysical properties of organic pcm through shape stabilization for thermal energy storage in buildings: A state of the art review," *Energy and Build.*, vol. 236, no. 1, p. 110799, 2021. [Online]. Available: https://doi.org/10.1016/j.enbuild.2021.110799

[31] A. Abhat, "Low temperature latent heat thermal energy storage: Heat storage materials," *Sol. Energy*, vol. 30, no. 4, p. 313–332, 1983. [Online]. Available: https://doi.org/10.1016/0038-092X(83)90186-X

[32] B. Zalba, J. M. Marın, L. F. Cabeza, and H. Mehling, "Review on thermal energy storage with phase change: materials, heat transfer analysis and applications," *Appl. Therm. Eng.*, vol. 23, no. 3, p. 251–283, 2003. [Online]. Available: https://doi.org/10.1016/S1359-4311(02)00192-8

[33] M. K. Rathod and J. Banerjee, "Thermal stability of phase change materials used in latent heat energy storage systems: A review," *Renew. Sustain. Energy Rev.*, vol. 18, p. 246–258, 2023. [Online]. Available: https://doi.org/10.1016/j.rser.2012.10.022

[34] T. Ma, J. Zhao, and Z. Li, "Mathematical modelling and sensitivity analysis of solar photovoltaic panel integrated with phase change material," *Appl. Energy*, vol. 228, p. 1147–1158, 2018. [Online]. Available: https://doi.org/10.1016/j.apenergy.2018.06.145

[35] P. H. Biwole, P. Eclache, and F. Kuznik, "Phase-change materials to improve solar panel's performance," *Energy Build.*, vol. 62, p. 59–67, 2013. [Online]. Available: https://doi.org/10.1016/j.enbuild.2013.02.059

[36] Z. Jiang, F. Jiang, C. Li, G. Leng, X. Zhao, Y. Li, T. Zhang, G. Xu, Y. Jin, C. Yang, and Y. Ding, "A form stable composite phase change material for thermal energy storage applications over 700 °c," *Applied Sciences*, vol. 9, no. 5, 2019. [Online]. Available: https://doi.org/10.3390/app9050814

[37] Y. Chen, J. Sun, P. Jiang, Z. Chai, B. Zhang, and J. Li, "Review on porous ceramic-based form-stable phase change materials preparation', enhance thermal conductivity and application," *ChemBioEng Reviews*, vol. 10, no. 6, pp. 941–958, 2023. [Online]. Available: https://doi.org/10.1002/cben.202300023

[38] Jacobson and J. Smialek, "Corrosion pitting of sic by molten salts," *J. The Electrochemical Society*, vol. 133, no. 12, pp. 2615–2621, 1986. [Online]. Available: https://doi.org/10.1149/1.2108490

[39] Q. Chen, H. Wang, H. Gao, X. Wang, and B. Ma, "Effects of porous silicon carbide supports prepared from pyrolyzed precursors on the thermal conductivity and energy storage properties of paraffin-based composite phase change materials," *Journal of Energy Storage*, vol. 56, no. PartB, p. 106046, 2022. [Online]. Available: https://doi.org/10.1016/j.est.2022.106046

[40] Z. Yu, X. Li, J. Wang, and S. Zhang, "form-stable na2co3-nacl/mullite phase change composite with sic enhanced thermal conductivity for high temperature thermal storage," *Journal of Energy Storage*, vol. 87, p. 111511, 2024. [Online]. Available: https://doi.org/10.1016/j.est.2024.111511

[41] O. Adesusi, O. Adetunji, S. Kuye, S. Ipadeola, S. I. Kuye, A. I. Musa, T. J. Erinle, and O. B. Gbadamosi-Olatunde, "Comprehensive review of the materials degradation phenomena in solid–liquid phase change materials for thermal energy storage," *International Journal of Thermofluids*, vol. 18, no. 2, p. 100360, 2023. [Online]. Available: https://doi.org/10.1016/j.ijft.2023.100360

[42] R. T. DeHoff, *Thermodynamics in Materials Science (2nd ed.)*. Taylor and Francis Group, 2006, no. ISBN 9780849340659.

[43] Z. Jiang, F. Jiang, and C. L. et al, "A form stable composite phase change material for thermal energy storage applications over 700 ∘c," *journal applied sciences*, vol. 9, no. 5, p. 814, 2019. [Online]. Available: https://doi.org/10.3390/app9050814

[44] J. Adler, "Ceramic diesel particulate filters," *I.J. Applied Ceramic Technology*, vol. 2, no. 6, pp. 429–439, 2005. [Online]. Available: https://doi.org/10.1111/j.1744-7402.2005.02044.x

[45] A. J. Pyzik and C. G. Li, "New design of a ceramic filter for diesel emission control applications," *I.J. Applied Ceramic Technology*, vol. 2, no. 6, pp. 440–451, 2005. [Online]. Available: https://doi.org/10.1111/j.1744-7402.2005.02045.x

[46] K. Koumoto, M. Shimohigoshi, T. Shunji, and H. Yanagida, "Thermoelectric energy conversion by porous sic ceramics," *Journal of Materials Science Letters*, vol. 6, no. 2, p. 1453–1455, 1987. [Online]. Available: https://doi.org/10.1007/BF01689320

[47] M. Fukushima, "Microstructural control of macroporous silicon carbide," *Journal of the Ceramic Society of Japan*, vol. 121, no. 1410, p. 162–168, 2013. [Online]. Available: https://doi.org/10.2109/jcersj2.121.162

[48] D. Das and N. Kayal, "Thermal shock resistance of porous silicon carbide ceramics prepared using clay and alumina as additives," *Transactions of the Indian Ceramic Society*, vol. 78, no. 3, pp. 165–171, 2019. [Online]. Available: https://doi.org/10.1080/0371750X.2019.1665478

[49] M. J. Huang, P. C. Eames, and B. Norton, "Thermal regulation of building-integrated photovoltaics using phase change materials," *Int. J. Heat Mass Transf.*, vol. 47, no. 12–13, p. 2715–2733, 2004. [Online]. Available: https://doi.org/10.1016/j.ijheatmasstransfer.2003.11.015

[50] S. Sharma, L. Micheli, W. Chang, A. A. Tahir, K. S. Reddy, and T. K. Mallick, "Nano-enhanced phase change material for thermal

management of bicpv," *Appl. Energy*, vol. 208, p. 719–733, 2017. [Online]. Available: https://doi.org/10.1016/j.apenergy.2017.09.076

[51] S. Nishad, Z. Ahmad, and I. Krupa, "Enhancement of photovoltaic module performance by thermal management using shape-stabilized pcm composites," *Sol. Energy Mater. Sol. Cells*, vol. 273, p. 112948, 2024. [Online]. Available: https://doi.org/10.1016/j.solmat.2024.112948

[52] Y. Xu, Q. Ren, Z.-J. Zheng, and Y.-L. He, "Evaluation and optimization of melting performance for a latent heat thermal energy storage unit partially filled with porous media," *Appl. Energy*, vol. 193, no. 2, p. 84–95, 2017. [Online]. Available: https://doi.org/10.1016/j.apenergy.2017.02.019

[53] H. I. Mohammed, P. Talebizadehsardari, J. M. Mahdi, A. Arshad, A. Sciacovelli, and D. Giddings, "Improved melting of latent heat storage via porous medium and uniform joule heat generation," *J. Energy Storage*, vol. 31, no. 2, p. 101747, 2020. [Online]. Available: https://doi.org/10.1016/j.est.2020.101747

[54] A. Arshad, M. Jabbal, P. T. Sardari, M. A. Bashir, H. Faraji, and Y. Yan, "Transient simulation of finned heat sinks embedded with pcm for electronics cooling," *Therm. Sci. Eng. Prog*, vol. 18, no. 2, p. 100520, 2020. [Online]. Available: https://doi.org/10.1016/j.tsep.2020.100520

[55] V. V. Calmidi and R. L. Mahajan, "Forced convection in high porosity metal foams," *J. Heat Transf.*, vol. 122, no. 3, p. 557–565, 2000. [Online]. Available: https://doi.org/10.1115/1.1287793

[56] A. Hasan, J. Sarwar, H. Alnoman, and S. Abdelbaqi, "Yearly energy performance of a photovoltaic-phase change material (pv-pcm) system in hot climate," *Sol. Energy*, vol. 146, no. 2, p. 417–429, 2017. [Online]. Available: https://doi.org/10.1016/j.solener.2017.01.070

[57] Éponge Métallique Poreuse En Cuivre Mousse. [Online]. Available: https://www.made-in-china.com

[58] S. Nishad, Z. Ahmad, and I. Krupa, "Enhancement of photovoltaic module performance by thermal management using shape-stabilized pcm composites," *Sol. Energy Mater. Sol. Cells*, vol. 273, p. 112948, 2024. [Online]. Available: https://doi.org/10.1016/j.solmat.2024.112948

[59] E. Deniz and S. Çınar, "Energy, exergy, economic and environmental (4e) analysis of a solar desalination system with humidification-dehumidification," *Energy Convers. Manag.*, vol. 126, no. 2, p. 12–19, 2016. [Online]. Available: https://doi.org/10.1016/j.enconman.2016.07.064

[60] H. Eggleston, L. Buendia, K. Miwa, T. Ngara, and K. Tanabe, "Guidelines for national greenhouse gas inventories, energy. prepared by the national greenhouse gas inventories programme," *IPCC Guidelines for National Greenhouse Gas Inventories*, vol. 2, 2006. [Online]. Available: https://www.ipcc-nggip.iges.or.jp/public/2006gl/vol2.html

[61] IEA, "Global energy review 2025," *IEA (2025)*, vol. IEA, Paris, 2023. [Online]. Available: https://www.iea.org/reports/global-energy-review-2025

[62] V. R. Voller and C. Prakash, "A fixed grid numerical mode ing methodology for convection-diffusion mushy region phase-change problems," *International Journal of Heat and Mass Transfer*, vol. 30, no. 8, pp. 1709–1719, 1987. [Online]. Available: https://doi.org/10.1016/0017-9310(87)90317-6

[63] C. Ji, Z. Qin, Z. Low, S. Dubey, F. H. Choo, and F. Duan, "Non-uniform heat transfer suppression to enhance pcm melting by angled fins," *Appl. Therm. Eng.*, vol. 129, p. 269–279, 2018. [Online]. Available: https://doi.org/10.1016/j.applthermaleng.2017.10.030

[64] E. Anastasiou, K. O. Lorentz, G. J. Stein, and P. D. Mitchell, "Prehistoric schistosomiasis parasite found in the middle east," *Lancet Infect. Dis.*, vol. 14, no. 7, p. 553–554, 2014. [Online]. Available: https://doi.org/10.1016/S1473-3099(14)70794-7

[65] Thermal Conductive Materials. [Online]. Available: https://www.made-in-china.com

[66] B. Kamkari, H. Shokouhmand, and F. Bruno, "Experimental investigation of the effect of inclination angle on convection-driven melting of phase change material in a rectangular enclosure," *Int. J. Heat Mass Transf.*, vol. 72, p. 186–200, 2014. [Online]. Available: https://doi.org/10.1016/j.ijheatmasstransfer.2014.01.014

[67] C. Y. Zhao, W. Lu, and Y. Tian, "Heat transfer enhancement for thermal energy storage using metal foams embedded within phase change materials (pcms)," *Sol. Energy*, vol. 84, no. 8, p. 1402–1412, 2010. [Online]. Available: https://doi.org/10.1016/j.solener.2010.04.022

[68] Z. Liu, Y. Yao, and H. Wu, "Numerical modeling for solid–liquid phase change phenomena in porous media: Shell-and-tube type latent heat thermal energy storage," *Appl. Energy*, vol. 112, pp. 1222–1232, 2013. [Online]. Available: https://doi.org/10.1016/j.apenergy.2013.02.022

How to cite this article:
Khaldi Sabrina, Driss Nehari, Abdelkader Youcefi, and Bachir Imin (2025). 'Improving the performance of a photovoltaic panel using phase change materials enhanced with metal foams', Al-Qadisiyah Journal for Engineering Sciences, 18(4), pp. 378-390. https://doi.org/10.30772/qjes.2025.161063.1581